Author: Brouwer, Margot
Title: Studying dark matter using weak gravitational lensing : from galaxies to the cosmic web
Date: 2017-12-20

1 Introduction

"A cosmic mystery of immense proportions, once seemingly on the verge of solution, has deepened and left astronomers and astrophysicists more baffled than ever. The crux of the riddle is that the vast majority of the mass of the universe seems to be missing. Or, more accurately, it is invisible to the most powerful telescopes on earth or in the heavens, which simply cannot detect all the mass that ought to exist in even nearby galaxies." – William J. Broad, New York Times (September 11, 1984).

In these three sentences, New York Times reporter William Broad describes what is still one of the biggest mysteries in modern cosmology. Over the past decades, astronomers have found evidence that all known types of matter - stars, planets, gas, dust and even exotic objects like black holes and neutrino's - only constitute $\sim 20\%$ of all mass in the universe. The other 80% is thought to consist of a hypothetical and invisible substance called dark matter. So far, however, all evidence is based exclusively on its gravitational interaction, either trough the dynamics of normal visible (often called 'baryonic') matter, or through the deflection of light in curved spacetime. This latter approach, called gravitational lensing, is a unique way to probe the distribution of dark matter without making any assumptions on its dynamical state (such as virial equilibrium in clusters), and on scales larger than the extent of baryons (e.g. outside the visible disks of galaxies). With this thesis, I hope to increase our knowledge of the distribution and behaviour of dark matter using weak gravitational lensing. On scales ranging from individual galaxies to groups, and even to large-scale structure, I study the link between baryonic and dark matter with the ultimate goal of gleaning some insight into its possible nature.

1.1 Dark Matter

1.1.1 Discovery and evidence

The first evidence of Dark Matter (DM) was found by Zwicky (1933), who used the virial theorem to study dynamics of galaxies in the Coma cluster. He found that the mass density of the cluster must be at least 400 times larger than expected from its luminous contents, and suggested 'Dunkle Materie' as a possible cause. At this time, he used this term to indicate *baryonic* DM, such as cold non-radiating gas, planets or compact objects. His findings were substantiated by Kahn and Woltjer (1959) who studied the dynamics of the Local Group. More than 20 years later Rubin (1983), who studied the spectra of galactic optical disks and found their rotation curves flattened, brought DM to a wider attention. By that time Freeman (1970) had already found the flattening of rotation curves in the disks of spiral and $\mathrm{S0}$ galaxies, and Bosma (1981) at scales far beyond the disks (using hydrogen profiles). All their research combined showed that, on scales ranging from individual galaxies to clusters, the gravitational potential found by applying Newtonian dynamics was too deep to be generated by the observed luminous matter. This 'excess gravity' was expected to arise from the DM coined by Zwicky, either in the form of baryonic or non-baryonic particles.

Some astrophysicists posed an alternative explanation to this problem: that the Newtonian laws of gravity are not accurate at these large scales. This could be solved by an adjustment of the laws of gravity, such as implemented by Milgrom (1983) who conceived Modified Newtonian Dynamics (MoND). Based on empirical evidence from galactic rotation curves, MoND adjusts Newton's second law of motion, $F = m\,a$, which relates the force F on a mass m to its acceleration a. Below a certain critical acceleration a_0 the Newtonian force F_{N} is adjusted as follows: $F_{\mathrm{N}} = m\,a_{\mathrm{N}} = m\,a^2/a_0$, which reproduces the observed flattening of the rotation curves. The necessary value of a_0 to describe these observations turns out to lie close to $c\,H_0$, where c is the speed of light and H_0 the present expansion rate of the universe. However, MoND's prediction for the mass of clusters, based on their visible baryonic content, is still too low without invoking some form of DM (Aguirre et al. 2001), such as massive neutrinos (Sanders 2003; Pointecouteau and Silk 2005).

During and after the conception of MoND, the COBE (Mather 1982) and WMAP (Spergel et al. 2003) missions produced accurate temperature maps of the Cosmic Microwave Background (CMB) radiation: the photons that were released during the era of recombination, ~ 380.000 years after the Big Bang. The spectrum of the observed temperature fluctuations revealed the acoustic oscillations present in the primordial plasma, caused by the interplay between light, mass and the expansion of the universe. As a non-relativistic theory, MoND could not explain the structure of the CMB. A relativistic generalization of MoND named TeVeS was created by Bekenstein (2004), but it is disputed whether a TeVeS model, even with the inclusion of massive neutrinos, can reproduce the observed structure formation and CMB power spectrum (Skordis et al. 2006; Xu et al. 2015).

So far, the theoretical framework that explains these observations best is the ΛCDM model. In this model, the majority of the energy density in the universe (68.5% as measured by Planck XIII 2016) consists of a cosmological constant Λ, which causes the Universe to expand at an accelerating rate. Only 4.9% of the energy density consists of normal baryonic matter. The remaining 26.6% of the universe's energy density constitutes the discussed 'missing mass', which consists of cold DM particles. Here 'cold' means that the DM was non-relativistic when it decoupled from baryonic matter. This is necessary since relativistic DM would have washed away the density fluctuations existing in the early universe, which originated from primordial quantum fluctuations. This would be inconsistent with our current observations, since these initial density variations accreted mass to form the Large Scale Structure (LSS) observed by galaxy redshift surveys today. Independent evidence that these DM particles cannot have a baryonic origin can be obtained from the abundances of primordial light elements (Deuterium, Lithium and several Helium isotopes), which were created during the first few minutes after the Big Bang (Alpher et al. 1948). The reconstruction of this period of 'Big Bang Nucleosynthesis', based on the principles of nuclear physics, shows that the baryon density is $\sim 5\%$ of the universe's total energy density (Pettini and Bowen 2001). This shows again that the baryonic density is much smaller than the total energy and matter density inferred from CMB observations.

But the most striking indication that DM might have a particle nature (as opposed to a modification of gravity) comes from weak gravitational lensing. The study by Clowe et al. (2006) of the Bullet Cluster, an ongoing merger of two colliding galaxy clusters, reveals that the major component of the gravitational potential resides at a different location than the major component of the baryonic mass (see Figure 1.1). The latter consists of hot gas, and is observed through its X-ray emission, while the former component is observed through the gravitational distortion of light from background galaxies. This famous example shows that weak gravitational

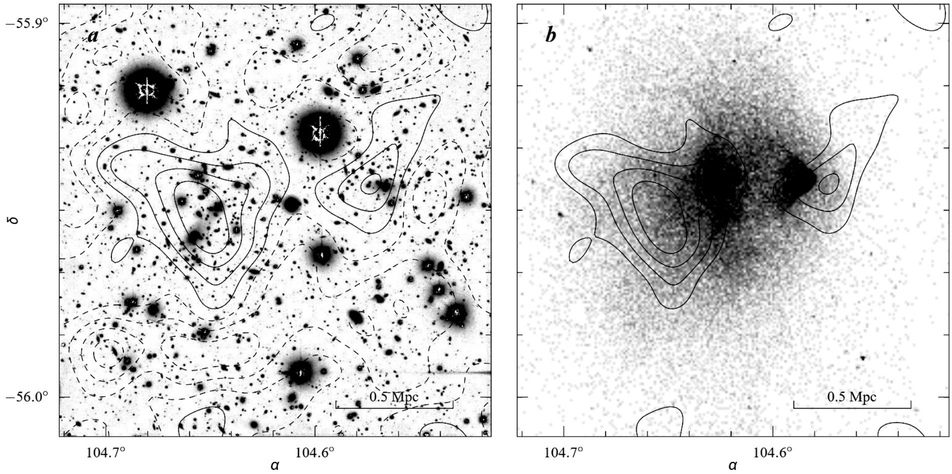

Figure 1.1: (a) An optical image of the galaxies in cluster 1E0657-56, or 'the Bullet Cluster', overlayed with the mass contours measured through weak gravitational lensing. The mass peak of the right subcluster (the 'bullet') approximately coincides with its galaxy concentration. This suggests that, like the galaxies, DM is collisionless. (b) An X-ray image of the Bullet Cluster, overlayed with the same mass contours. The X-ray is emitted by hot cluster gas, which constitutes the main baryonic mass component. The main dark and baryonic mass distributions do not coincide, suggesting that DM can exist separately from baryonic matter. Originally published in Markevitch et al. (2006).

lensing is a unique probe of the distribution of DM, independent of its dynamical state. It allows us to obtain a deeper understanding of its behaviour and relation to baryonic matter, which can ultimately lead us closer to the discovery of its fundamental nature.

1.1.2 Cosmic structure

The relation between dark and baryonic matter, which is one of the main themes of this thesis, can be studied on a wide range of scales: from individual galaxies to small groups, large clusters, and even to largest known structure in the universe: the 'cosmic web'. The exact nature of the relation between dark and baryonic matter at each scale, depends on how these structures formed. The first seeds of cosmic structure were established during the epoch of inflation: a period that took place $\sim 10^{-36}$ to 10^{-32} seconds after the Big Bang, in which space expanded exponentially (Guth 1981; Sato 1981). The 'inflaton field', which theoretically caused this exponential expansion, contained microscopic quantum fluctuations that were subsequently magnified to cosmic sizes. After 're-heating', the decay of the inflaton field into matter and radiation, these macroscopic fluctuations remained as overdensities. The period of superluminal expansion also explains why our current universe appears homogeneous, isotropic, flat, and devoid of relic exotic particles (such as magnetic monopoles).

The thermalization of the universe is followed by the radiation-dominated era, where most of the energy density was contained by photons. During this epoch, the gravitational growth of structure was impeded by the rapid expansion of the universe. But while space continued to expand, the energy density of radiation diluted faster than that of matter, due to the redshifting of the photons. Around $47,000$ years after the Big Bang, the energy density in radiation and matter had equalized, marking the beginning of the matter-dominated era. At the start of this era, baryonic matter was still ionized due to the high temperatures (> 3000 Kelvin), and could not collapse due too radiation pressure. DM, however, which is not affected by radiation pressure, could now start to gravitationally collapse. Structure formation models pose that the primordial density perturbations grew into a network of roughly spherical DM halos (Peebles and Yu 1970). This early formation of structure, where density contrasts are still small, can be analytically described using the 'linear power spectrum'.

Only after $\sim 380,000$ years the universe had cooled enough to allow for the recombination of electrons and protons into neutral hydrogen, which disconnected the baryonic matter from the photon pressure. The photons that escaped during recombination are currently observed as the CMB. In the ΛCDM paradigm, the total mass of the baryonic matter component is sub-dominant to that of DM (less than $\sim 1/5$ its mass), causing its spatial structure to broadly follow that of the DM through gravitational attraction. A galaxy forms when baryonic matter is pulled into the potential well of a DM halo, and cools at its centre (Blumenthal et al. 1984). Since baryonic matter can lose potential energy through radiative cooling (whereas DM cannot) the galaxies thus formed have a radius ~ 100 times smaller than that of the DM halo, which can only collapse through virialization.

As the density contrast of DM increases through further gravitational collapse, later stages of structure formation become impossible to describe analytically. Computational N-body simulations that incorporate Newtonian gravity are currently the most convenient method of studying structure formation at later times. The ΛCDM model constitutes the basis for extensive N-body simulations (containing $\sim 10^9$ particles), such as the Millennium Simulation (Springel et al. 2005b) and the EAGLE project (Schaye et al. 2015), which provide excellent predictions for LSS formation. These simulations show a hierarchical clustering of DM halos, forming combined structures from small groups to big clusters. On the largest scales, they exhibit a web-like structure formed by filaments and sheets of DM. At the intersection of these structures, the DM halos coalesce into giant superclusters, while in between there exist immense underdense regions named voids.

As the DM structure evolves the baryonic matter, consisting primarily of galaxies and gas, follows. On the level of a single galaxy inhabiting a DM halo, we observe mergers that increase both the halo and galaxy mass (White and Frenk 1991). If the local number density of halos (within a few Mpc range) is high, the increased merger rate is expected to boost the average galaxy and halo mass (Bardeen et al. 1986; Cole and Kaiser 1989). On even larger scales we observe that, through gravitational attraction, the cosmic DM web acts as a skeleton to the baryonic matter, which primarily consists of gas clouds, galaxies, clusters and superclusters (Bond et al. 1986). The reflection of the cosmic DM web in the large-scale distribution of galaxies can be observed by large scale redshift surveys, such as the 2dF Galaxy Redshift Survey (2dFGRS, Colless et al. 2001) and the Sloan Digital Sky Survey (SDSS, Abazajian et al. 2009). If and how this LSS affects galaxies and halos is still subject to debate (Hahn et al. 2009; Ludlow and Porciani 2011; Alonso et al. 2015), but so far no observational evidence for such effects has been found (Darvish et al. 2014; Alpaslan et al. 2015; Eardley et al. 2015).

Over the course of this thesis, we study the relation between galaxies and halos on the scale of individual galaxies and galaxy groups, we try to measure the effect of the local and large scale (cosmic web) density distribution on galaxies and haloes, and we measure the interplay between galactic and DM structures at the scale of the cosmic web. All observations of the aforementioned DM distributions are based on the weak gravitational lensing method.

1.2 Weak gravitational lensing

1.2.1 The weak lensing method

In Einstein's theory of General Relativity (GR), gravitational force is equivalent to the curvature of space-time. Based on this theory, he could calculate the deflection of light that travels through a part of space-time which is curved by a specific mass. Most famously, he predicted this deflection for the light of distant stars by the Sun, which was measured by Sir Arthur Eddington in 1919. The observation of stars close to the sun (in projection) could only be performed during a total eclipse, which required an expedition to the African island of Principé. Eddington confirmed Einstein's prediction, which provided both the theory of GR and themselves with instant credibility and fame.

This deflection of light by gravity is called 'gravitational lensing', and has become a widely used method to measure mass distributions in the universe. In this thesis, we use gravitational lensing to measure the total (baryonic + dark) mass distribution around galaxies, galaxy groups and larger structures. This is done specifically through 'weak gravitational lensing' (WL) of the light from background galaxies. When both the foreground lenses and the background sources are galaxies, this method is called 'galaxy-galaxy lensing' (for a more elaborate discussion, see e.g. Bartelmann and Schneider 2001; Schneider et al. 2006).

The fundamental principle behind lensing is illustrated in Fig. 1.2, where the light from one background source is deflected by a foreground point mass which acts as a gravitational lens. Because the angular diameter distances $D_{\rm l}$ and $D_{\rm s}$ to the lens and the source are very large compared to the width of the lens along the 'line of sight' (LOS), we can apply the 'thin lens approximation'. Instead of taking the full curved path of the light ray into account we can assume that the light is instantaneously deflected at the lens plane, where it passes the centre of the lens at a projected radial distance R. In GR, the deflection angle $\hat{\alpha}$ of the light ray is related to the mass M of the lens as:

$$\hat{\alpha} = \frac{4GM}{c^2 R}\,, \tag{1.1}$$

where c denotes the speed of light and G the gravitational constant. Also, the true position of the source with respect to the LOS, $\eta = \beta\, D_{\rm s}$, is related to its apparent position $R = \theta\, D_{\rm l}$ as:

$$\eta = \frac{D_{\rm s}}{D_{\rm l}} R - D_{\rm ls}\hat{\alpha}\,. \tag{1.2}$$

This can be rewritten as the 'lens equation':

$$\beta = \theta - \frac{D_{\rm ls}}{D_{\rm s}}\hat{\alpha} \equiv \theta - \alpha, \tag{1.3}$$

where α is the 'reduced deflection angle', scaled by the distance $D_{\rm ls}$ between the lens and the source.

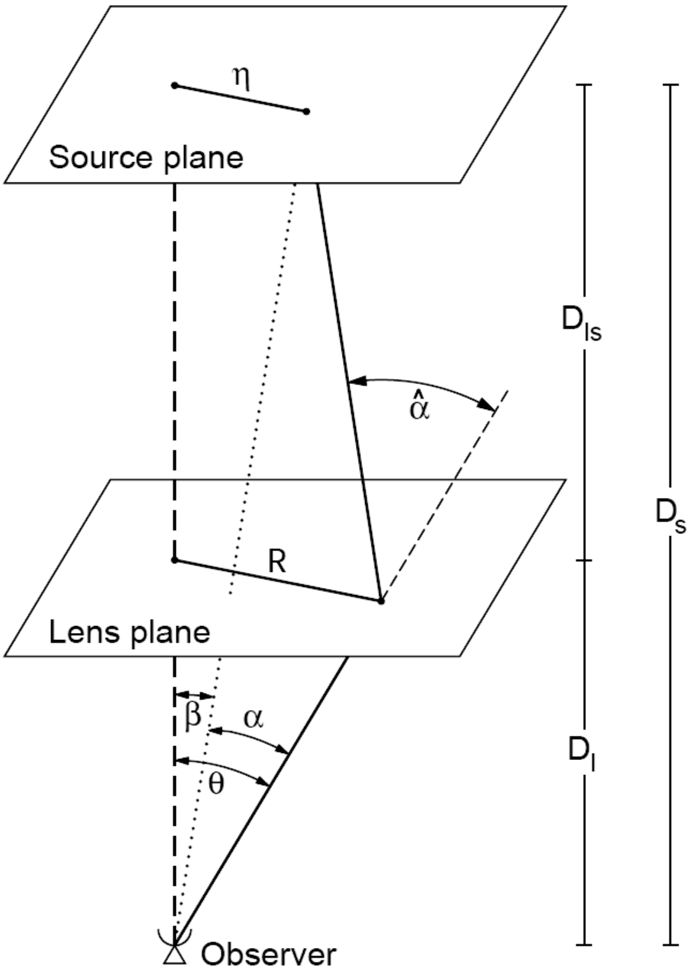

Figure 1.2: A schematic view of gravitational lensing. The dashed line shows the 'line of sight' (LOS), which goes from the observer through the center of the lens to the source plane. At projected distance η from the LOS, a source emits a light ray which is deflected at an angle $\hat{\alpha}$. This means it is now observed at a projected distance R from the center of the lens, instead of its true position. For an extended source, this results in a tangential shape distortion with respect to the lens center. This distortion, called shear, is a probe of the surface density distribution $\Sigma(R)$ of the lens. Originally published in Bartelmann & Schneider (2001).

Instead of a point mass, we can also consider a density distribution $\rho(R, z, \varphi)$. This distribution is represented in cylindrical coordinates, where z is the LOS direction and φ the angle with respect to the lens centre (in the lens plane). If we assume an azimuthally symmetric mass distribution we can integrate over φ, such that the density only depends on R and z. We can now represent the mass M from Eq. 1.1 as:

$$M = \int \rho(R, z, \varphi)\, R\, \mathrm{d}R\, \mathrm{d}z\, \mathrm{d}\varphi \;= 2\pi \int \rho(R, z)\, R\, \mathrm{d}R\, \mathrm{d}z\,. \tag{1.4}$$

However, the gravitational lensing method only provides information on the density integrated along the LOS, which is defined as the projected surface mass density:

$$\Sigma(R) = \int \rho(R, z)\, \mathrm{d}z\,. \tag{1.5}$$

We combine Eq. 1.4 and 1.5 to express the reduced deflection angle from Eq. 1.3 in terms of the surface density:

$$\begin{aligned}\alpha = \hat{\alpha}\,\frac{D_\mathrm{ls}}{D_\mathrm{s}} = \frac{4G}{c^2 R}\frac{D_\mathrm{ls}}{D_\mathrm{s}}\, 2\pi \int \Sigma(R)\, R\, \mathrm{d}R \;=& \\ \frac{2}{D_\mathrm{l} R} \int \frac{4\pi G}{c^2}\frac{D_\mathrm{l}\, D_\mathrm{ls}}{D_\mathrm{s}}\, \Sigma(R)\, R\, \mathrm{d}R \;\equiv\; & \frac{2}{D_\mathrm{l} R} \int \frac{\Sigma(R)}{\Sigma_\mathtt{crit}}\, R\, \mathrm{d}R\,.\end{aligned} \tag{1.6}$$

Here $\Sigma_\mathtt{crit}$ is the critical density surface mass density:

$$\Sigma_\mathtt{crit} = \frac{c^2}{4\pi G}\frac{D_\mathrm{s}}{D_\mathrm{l}\, D_\mathrm{ls}}\,, \tag{1.7}$$

which is the inverse of the lensing efficiency: a geometrical factor that determines the strength of the lensing effect based on the distances between the lens, the source and the observer. Defining the dimensionless surface mass density $\kappa(R) \equiv \Sigma(R)/\Sigma_\mathtt{crit}$ and remembering that $R = \theta\, D_\mathrm{l}$, the lens equation (Eq. 1.3) now becomes:

$$\beta(\theta) = \theta(1 - \alpha(\theta)/\theta) = \theta(1 - \langle\kappa\rangle) \tag{1.8}$$

where $\langle\kappa\rangle$ is the average dimensionless surface density inside radius R (or angle θ):

$$\langle\kappa(R)\rangle = \frac{2}{\theta\, D_\mathrm{l} R} \int \frac{\Sigma(R)}{\Sigma_\mathtt{crit}}\, R\, \mathrm{d}R = \frac{2}{\theta^2} \int \kappa(\theta)\, \theta\, \mathrm{d}\theta = \frac{\alpha(\theta)}{\theta}\,. \tag{1.9}$$

In this thesis the lensed sources are galaxies, which have extended 2D images. As can already be seen from Eq. 1.1, the amount of deflection depends on the distance vector $\vec{R}$ to the lens. When lensing affects an extended source, this causes a differential distortion of the image. The intrinsic surface brightness distribution $I_{\rm int}(\vec{\beta})$ (in the source plane) is mapped to the observed distribution $I_{\rm obs}(\vec{\theta})$ (in the lens plane) through the 2D coordinate transformation $\vec{\beta}(\vec{\theta})$:

$$I_{\rm obs}(\vec{\theta}) = I_{\rm int}[\vec{\beta}(\vec{\theta})] \tag{1.10}$$

In the case of our work, the size of the background sources is negligible compared to the angular scale on which the mass density of the lens changes. This means that the coordinate transformation can be linearised as follows:

$$\vec{\beta}(\vec{\theta}) = \vec{\beta}_0 + \frac{\delta\vec{\beta}}{\delta\vec{\theta}}(\vec{\theta} - \vec{\theta}_0)\,, \tag{1.11}$$

where β_0 and θ_0 are corresponding points in the source and lens plain respectively. The image distortion $\delta\vec{\beta}/\delta\vec{\theta}$ can be derived by applying the Jacobian to β (from Eq. 1.8) as follows:

$$\frac{\delta\vec{\beta}}{\delta\vec{\theta}} = \frac{\delta([1-\langle\kappa\rangle]\vec{\theta})}{\delta\vec{\theta}} = (1-\langle\kappa\rangle)\begin{bmatrix}1 & 0\\ 0 & 1\end{bmatrix} - \frac{\delta\langle\kappa\rangle}{\delta\theta}\begin{bmatrix}\theta_1^2 & \theta_1\theta_2\\ \theta_1\theta_2 & \theta_2^2\end{bmatrix}/|\theta|\,, \tag{1.12}$$

where θ_1 and θ_2 are the two components of the location vector $\vec{\theta}$ of the source with respect to the equatorial coordinate system. Since we are considering an azymuthally symmetric lens, it is convenient to express this location in terms of its angle ϕ with respect to the centre of the lens: $\vec{\theta} = |\theta|(\cos(\phi)\,,\, \sin(\phi))$. Furthermore, the derivative of $\langle\kappa(\theta)\rangle$ can be solved using the third term of Eq. 1.9, which yields:

$$\frac{\delta\langle\kappa\rangle}{\delta\theta} = \frac{-2}{\theta}\left(\frac{2}{\theta^2}\int\kappa\,\theta\,{\rm d}\theta\right) + \frac{2}{\theta^2}\kappa\,\theta = \frac{2}{\theta}(\kappa - \langle\kappa\rangle)\,. \tag{1.13}$$

Using Eq. 1.13 and the definition of $\vec{\theta}$ to re-write Eq. 1.12 gives:

$$\frac{\delta\vec{\beta}}{\delta\vec{\theta}} = [1-\kappa+(\kappa-\langle\kappa\rangle)]\begin{bmatrix}1 & 0\\ 0 & 1\end{bmatrix} - (\kappa-\langle\kappa\rangle)\begin{bmatrix}2\cos^2(\phi) & 2\cos(\phi)\sin(\phi)\\ 2\cos(\phi)\sin(\phi) & 2\sin^2(\phi)\end{bmatrix} =$$
$$(1-\kappa)\begin{bmatrix}1 & 0\\ 0 & 1\end{bmatrix} + (\kappa-\langle\kappa\rangle)\begin{bmatrix}\cos(2\phi) & \sin(2\phi)\\ \sin(2\phi) & -\cos(2\phi)\end{bmatrix}\,. \tag{1.14}$$

Based on this equation we can define the 'tangential shear' γ_{t}, which is the distortion of the source (called 'shear') tangential to the direction of the lens' centre:

$$\gamma_{\mathrm{t}} = \langle\kappa\rangle - \kappa = -\gamma_1 \cos(2\phi) - \gamma_2 \sin(2\phi) = -\Re(\gamma\, e^{-2i\phi})\,, \tag{1.15}$$

where γ_1 and γ_2 are the components of the shear with respect to the equatorial coordinate frame, and:

$$\gamma = |\gamma| e^{2i\phi} = \gamma_1 + i\,\gamma_2\,. \tag{1.16}$$

In the case of WL studies the surface density is much smaller than Σ_{crit}, and the convergence $\kappa = \Sigma/\Sigma_{\mathrm{crit}} \ll 1$ in Eq. 1.14 is often ignored. Consequently, γ_{t} is the primary measure for the shape distortion used to estimate the gravitational lensing effect. At an angle of 45° with respect to γ_{t} we find the 'cross shear' γ_{x}, which is analogously defined as:

$$\gamma_{\mathrm{x}} = -\Im(\gamma\, e^{-2i\phi}) = \gamma_1 \sin(2\phi) - \gamma_2 \cos(2\phi)\,. \tag{1.17}$$

Because γ_{x} is not affected by lensing, it is very useful as a null test.

Using Eq. 1.15 the tangential shear $\gamma_{\mathrm{t}}(R)$ can be related to the Excess Surface Density (ESD) $\Delta\Sigma(R)$, which is defined as the surface mass density $\Sigma(R)$ at projected radial distance R from the lens centre, subtracted from the average density $\langle\Sigma(< R)\rangle$ within that radius:

$$\gamma_{\mathrm{t}}(R)\Sigma_{\mathrm{crit}} = [\langle\kappa(< R)\rangle - \kappa(R)]\Sigma_{\mathrm{crit}} = \langle\Sigma(< R)\rangle - \Sigma(R) \equiv \Delta\Sigma(R)\,. \tag{1.18}$$

To measure the tangential shear we observe the ellipticity ϵ of the background galaxies, which can be expressed in terms of the source's axis ratio b/a:

$$\epsilon = \frac{1 - b/a}{1 + b/a} e^{2i\phi}\,, \tag{1.19}$$

or as a two-component vector: $\vec{\epsilon} = |\epsilon|(\cos(2\phi)\,,\, \sin(2\phi))$. In reality, the observed ellipticity ϵ_{obs} of each source is a combination of both the shear γ and the intrinsic ellipticity ϵ_{int} of the galaxy. The unknown intrinsic ellipticities of galaxies are a limitation to all WL measurements, referred to as 'shape noise'. Although the amount of shape noise does not vary significantly between source populations with different properties (Leauthaud et al. 2007), it can depend on the shape measurement method. Therefore, the amount of shape noise is always carefully measured and propagated in the lensing errors. Compared to this noise, the shape distortion from lensing is so weak ($\sim 1\%$ of the intrinsic galaxy ellipticity) that it can only be measured statistically. This is achieved by accurately measuring the shapes of thousands of background galaxies in the field around a foreground mass distribution. In this way, we can measure the average shear by assuming that the intrinsic shapes are randomly oriented ($\langle\epsilon_{\rm int}\rangle = 0$), such that:

$$\langle\epsilon_{\rm obs}\rangle = \langle\epsilon_{\rm int} + \gamma\rangle = \langle\gamma\rangle\,. \tag{1.20}$$

By azimuthally averaging the sources' tangential shear components, the radial mass distribution of the lens can be reconstructed. To improve the signal-to-noise (S/N) even further, the radial lensing profile is averaged ('stacked') for large samples (hundreds to thousands) of lenses, often selected according to their observable properties. Combining the tangential shear for all lens-source pairs of a lens sample, binned in circular apertures of increasing radial distance R, results in the average shear profile $\langle\gamma_{\rm t}\rangle(R)$ of a lens sample. Using the distances to the lenses and sources, this quantity can in turn be translated to the ESD profile $\Delta\Sigma(R)$ of a lens sample.

1.2.2 The galaxy-galaxy lensing pipeline

The galaxy-galaxy lensing (GGL) software pipeline translates the measured distances and ellipticities of background galaxies (sources) from the Kilo-Degree Survey (KiDS, de Jong et al. 2013) into gravitational lensing profiles around foreground galaxies, groups or other mass distributions (lenses). This pipeline is used to perform the lensing measurements at the basis of the four chapters in this thesis (among other publications), and has the ability to calculate:

- the tangential and cross shear $\gamma_{\rm t}$ and $\gamma_{\rm x}$, as a function of the projected radial separation θ from the lens centre.
- the Excess Surface Density (ESD) as a function of the projected physical distance R from the lens centre.
- the additive and multiplicative bias correction of the lensing signal.
- the standard variance error on the lensing signal, based on the number and reliability of the source ellipticities.
- the analytical covariance matrix and errors, which are based on the contribution of each individual background source to the lensing signal and take into account the covariance related to sources that contribute to the profiles of multiple lenses.

- the bootstrap covariance matrix and errors, which are based on bootstrapping 1×1 deg survey tiles and take into account the contributions from sample variance and cosmic variance.

The pipeline can be operated through a user-friendly interface that allows users to specify the parameters of the lensing measurement: the type of lensing measurement, the type of error estimate, the values and unit of the radial bins around the lens, the values of the cosmological parameters, and the redshift range of the sources. The interface accepts any lens catalogue as input, and allows the user to select the lenses used for the analysis based on their measured observables. The lenses can be subjected to individual cuts and/or split into any number of bins. In case of the latter, the analytical and bootstrap covariance matrix will provide the covariance between the bins in observable, in addition to the covariance between the radial bins. One can also supply individual weights to scale the contribution of each lens to the signal, which will be taken into account into the calculation of the covariance matrix and the multiplicative bias correction.

After I created the first version of the pipeline for application to the KiDS DR2 data (KiDS, de Jong et al. 2015), the pipeline has been greatly improved and adjusted for the arrival of the KiDS DR3 data (de Jong et al. 2017) by Andrej Dvornik. Cristóbal Sifón has extended the pipeline with a module that allows the user to easily fit DM halo models to the output lensing profiles. The halo model framework is based on work by Marcello Cacciato, as applied in e.g. Cacciato et al. (2013). The most up-to-date version of the GGL pipeline is available for download through Github (`https://github.com/KiDS-WL/KiDS-GGL`).

1.3 Outline

This thesis describes our studies into the behaviour and distribution of DM through WL with KiDS. The studied structures (lenses) are mainly observed using the spectroscopic Galaxy And Mass Assembly survey (GAMA, Driver et al. 2011). The following subsections describe the contents of the individual chapters.

1.3.1 KiDS+GAMA: properties of galaxy groups

Chapter 2 contains the first WL study with the KiDS and GAMA surveys. This effort was made possible by the combined work of many contributors from both collaborations. My personal contribution was the construction and description of the GGL pipeline (see Sect. 1.2.2). This pipeline forms the basis of multiple KiDS-GAMA GGL papers, four of which are described below:

In Viola et al. (2015) we used gravitational lensing to study 'rich' galaxy groups (with 5 or more members). The groups, that have masses between $10^{13} < M < 10^{14.5}\,h^{-1}\mathrm{M}_{\odot}$, represent the most common galaxy environment in the universe. They were detected in the spectroscopic GAMA survey, and defined using a Friend-of-Friend algorithm that was calibrated using simulations. We split the ~ 1400 groups into bins based on their observable properties, and measured the ESD profile of each sub-sample. Interpreting the ESD profiles using a halo model framework allowed us to measure the group halo mass as a function of luminosity, velocity dispersion, (apparent) number of members, and fraction of group light in the central galaxy. Comparing this last relation to predictions from the Cosmo-OverWhelmingly Large Simulations (Cosmo-OWLS), we ruled out galaxy formation models without AGN feedback.

Sifón et al. (2015) used galaxy-galaxy lensing to study galaxies that are satellites in the aforementioned groups. Their main goal was to constrain the effect of 'halo stripping', the tidal removal of mass from satellite haloes by the halo of their host group. They separated the sample of $\sim 10,000$ satellites into three bins as a function of their projected distance to the group central, and measured the ESD of each subsample. Using the halo model framework, they measured the satellite halo mass as a function of its distance to the central, which is an estimator of the time since infall. They found no significant change in the stellar-to-halo mass relation of the satellites, which would signify halo stripping.

The goal of van Uitert et al. (2016) was to study the stellar-to-halo mass relation of galaxies, and whether it depends on group environment. By simultaneously fitting a halo model to the lensing profiles and the stellar mass function of galaxies, they obtained significantly better constraints. They found no large differences between the stellar-to-halo mass relation of all galaxies and those in rich groups, suggesting that the dependence on group environment is weak. For satellites, they found weak evidence of an increase in the halo mass fraction with stellar mass, which would imply halo stripping. However, impurities in the satellite sample could also cause this observation.

Dvornik et al. (2017) searched for signatures of 'halo assembly bias': the dependence of the distribution of DM haloes on any property besides their mass, such as formation time. They selected galaxy groups with different radial distributions of the satellite galaxies, which is a proxy for formation time. After measuring the ESD profiles of galaxy groups with 4 or more members, they measured their masses using the halo model framework. Using this method, they found no evidence of halo assembly bias on group scales.

Of these papers, I have included Viola et al. (2015) as a chapter in this thesis. The reason for including this paper specifically is that it was the very first KiDS-GAMA GGL paper, and that I was among the lead authors.

1.3.2 Galaxy halo masses in cosmic environments

In **Chapter 3**, which is based on Brouwer et al. (2016), we used the GGL pipeline and halo model framework to study the DM haloes of GAMA galaxies as a function of their large-scale environment. This environment consists of the cosmic web, a large network of mass structures that may influence the formation and evolution of DM haloes and the galaxies they host. The cosmic environments in our study were defined by Eardley et al. (2015) through a tidal tensor prescription, which finds the number of dimensions in which a volume is collapsing. Based on this number, the entire GAMA survey is divided into voids, sheets, filaments and clusters (called 'knots'). We measured the lensing profiles of the galaxies in these four environments and, through the halo model framework, modelled the contribution of central and satellite galaxies of groups, and the '2-halo' term caused by neighbouring groups. By correcting for the galaxies' stellar mass and 'local density' (the galaxy density within $4\,h^{-1}\,\mathrm{Mpc}$), we aimed to find the dependence of halo mass on the cosmic environments alone. Although the measured lensing signal was very sensitive to the local density through the amplitude of the 2-halo term, we found no direct dependence of the galaxy halo mass on local density or cosmic environment.

1.3.3 A weak lensing study of troughs

In **Chapter 4** we aimed to study the structure of the cosmic web itself, by measuring the lensing profiles of projected underdensities (troughs) and overdensities (ridges) in the KiDS galaxy number density distribution. Based on the definition of Gruen et al. (2016), we defined troughs with a projected radius $\theta_\mathrm{A} = \{5, 10, 15, 20\}$ arcmin. Through the amplitude A of the lensing profiles of troughs/ridges as a function of their galaxy number density, we explored the connection between their baryonic and total mass. We found that the skewness of the galaxy density distribution, which reveals non-linearities caused by the formation of cosmic structure, is reflected in the distribution of the total (baryonic + DM) mass distribution measured by lensing. The measured signal-to-noise (S/N) of the trough/ridge profiles as a function of galaxy number density allowed us to optimally stack their lensing signal, obtaining trough detections with a significance of $|S/N| = \{17.12, 14.77, 9.96, 7.55\}$. By splitting a volume limited galaxy sample into two redshift slices between $0.1 < z < 0.3$, we attempted to measure redshift evolution of troughs/ridges. The troughs were selected to have equal *comoving* lengths and radii at the different redshifts, to correct for the expansion of the universe. We found that, at these relatively low redshifts, there is no significant evolution. However, the MICE-GC mock catalogues to which we compared all our results, predict that at higher redshifts ($z \sim 0.6$) both troughs and ridges will exhibit signatures of structure evolution.

1.3.4 Lensing test of Verlinde's emergent gravity

Chapter 5, which is based on Brouwer et al. (2017), describes the first test of Emergent Gravity (EG, Verlinde 2017) through WL. The observable prediction of this theory, which proposes an alternative explanation to the excess gravity attributed to DM, is currently limited to the gravitational potential around spherically symmetric, static and isolated baryonic density distributions. We used the GAMA survey to find a sample of $33,613$ central galaxies that contain no other centrals within the projected radial distance range of our WL measurement: $0.03 < R < 3\,h_{70}^{-1}\mathrm{Mpc}$. Using the measured stellar masses of these galaxies we modelled their radial baryonic mass distributions, both as a simple point source and as an extended distribution that takes into account stars, cold gas, hot gas and satellites. For both models we predicted the lensing profiles in the EG framework, assuming that light is bent by a gravitational potential as in GR, and the background cosmology behaves like ΛCDM with a constant Hubble parameter. For the point mass model, this prediction is very similar to that from MoND (Milgrom 2013). We compared this prediction, which is fully determined by the baryonic mass distribution, to the WL profiles of isolated centrals in four different stellar mass bins. We found that the EG theory predicts our measurements equally well as an NFW profile with the halo mass as a free parameter, especially if we take these free parameters into account. After the publication of our research, several follow-up papers appeared that attempted to test the EG prediction on different scales. Ettori et al. (2017), who used X-ray data, weak lensing and galaxy dynamics to study the mass distributions of two galaxy clusters, found that EG reproduced the DM distribution needed to maintain the gas in pressure equilibrium beyond 1 Mpc from the cluster core, with a remarkable good match at radius $r \approx R_{500}$, but that it showed significant discrepancies (a factor 2–3) in the innermost 200 kpc. Lelli et al. (2017) studied the radial acceleration of disk galaxies, and found that EG was only consistent with the observed Radial Acceleration Relation for very low stellar mass-to-light ratios. Hees et al. (2017) showed that EG's predictions for the perihelion advancement of Solar System planets were discrepant with the data by seven orders of magnitude, although it can be disputed if this system can be considered static and isolated. Also in general these requirements of sphericity, staticity and isolation greatly inhibit the applicability of the EG prediction to cosmological observations and simulations. All in all, the theoretical framework of EG still has a long way to go before it can be considered as a viable competitor to the current ΛCDM model.